analytical chemistry

pubs.acs.org/ac Article

Multienzyme-Targeted Fluorescent Probe as a Biosensing Platform for Broad Detection of Pesticide Residues

Wu-Yingzheng Guo,[†] Yi-Xuan Fu,[†] Shi-Yu Liu, Long-Can Mei, Yao Sun, Jun Yin, Wen-Chao Yang,* and Guang-Fu Yang*

Cite This: *Anal. Chem.* 2021, 93, 7079−7085 Read Online

ACCESS | Metrics & More | Article Recommendations | Supporting Information

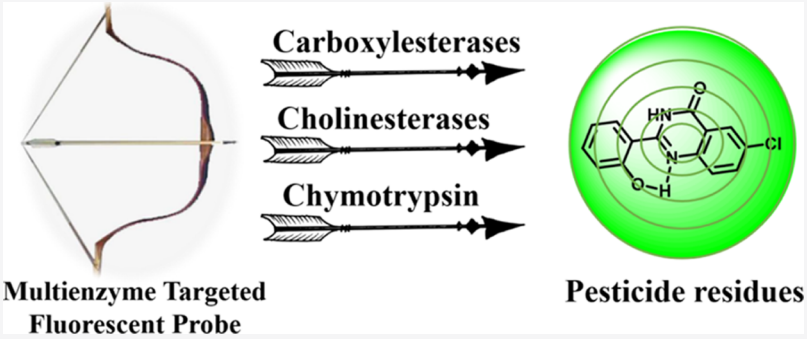

ABSTRACT: Pesticide residues, significantly hampering the overall environmental and human health, have become an increasingly severe issue. Thus, developing rapid, cost-effective, and sensitive tools for monitoring the pesticide residues in food and water is extremely important. Compared to the conventional and chromatographic techniques, enzyme inhibition-based biosensors conjugated with the fluorogenic probes provide effective alternative methods for detecting pesticide residues due to the inherent advantages including high selectivity and sensitivity, simple operation, and capability of providing in situ and real-time information. However, the detection efficiency of a single enzyme-targeted biosensor in practical samples is strongly impeded by the structural diversity of pesticides and their distinct targets. In this work, we developed a strategy of multienzyme-targeted fluorescent probe design and accordingly obtained a novel fluorescent probe (named as **3CP**) for detecting the presence of wide variety of pesticides. The designed probe **3CP**, targeting cholinesterases, carboxylesterases, and chymotrypsin simultaneously, yielded intense fluorescence in the solid state upon the enzyme-catalyzed hydrolysis. It showed excellent sensitivity against organophosphorus and carbamate pesticides, and the detection limit for dichlorvos achieved 1.14 pg/L. Moreover, it allowed for the diffusion-resistant in situ visualization of pesticides in live cells and zebrafish and the sensitive measurement of organophosphorus pesticides in fresh vegetables, demonstrating the promising potential for tracking the pesticide residues in environment and biological systems.

INTRODUCTION

Pesticides, which are originally designed to be toxic to pests, play important roles in public health such as killing vectors (like mosquitoes) of disease and in agriculture to protect crop yields.[1] However, overdose of the residual pesticides in food and water, mostly caused by the improper or excessive use of various pesticides such as the organophosphorus, carbamate, and pyrethroid pesticides, has raised a number of health-related problems and environmental damage all over the world.[2−6] In this regard, World Health Organization has classified pesticides into various classes based on their toxicity, and those pesticides with significant toxicity were strictly banned to be used any longer.[7] However, the continuous excessive and uncontrolled use of low-toxicity pesticides are still harmful to both environment and human health, which promoted the development of numerous detection methods for pesticide residues.[7−10]

At present, several conventional techniques are currently available for assessing the pesticide residues, including gas chromatography, high-performance liquid chromatography (HPLC), mass spectrometry (MS), and electrophoresis.[11−16] Most of them are usually employed to analyze pesticide residues in laboratories, which require complicated operation skills and expensive equipment and are also time-consuming. Thus, there is an urgent need for an immediate, simple, and effective technique for real-time detection of residual pesticides. Biosensors have attracted more attention due to

Received: February 5, 2021
Accepted: April 20, 2021
Published: April 28, 2021

https://doi.org/10.1021/acs.analchem.1c00553
Anal. Chem. 2021, 93, 7079−7085

the high signal-to-noise ratio, excellent sensitivity, and easy operation.[17−20] They could employ different biological elements such as proteins, enzymes, DNA, cells, and even whole live organisms as recognition hosts to detect different pesticides as guests.[21−25] Among them, enzyme inhibition-based biosensors integrating with optical probes received tremendous attention owning to their typical advantages such as high sensitivity and selectivity, simple operation, fast response, and good stability.[7,26−30] However, the real-time detection of pesticide residues by such enzyme-based biosensors has been severely limited by substantial structure diversity of pesticides and their diverse action modes. Besides, the diffusion/dilution of the fluorescent signal for the enzyme-activated fluorescent probes impedes the in situ detection and differentiation, which has never been considered for monitoring pesticides in the past.[31]

To address the abovementioned issues, here, we developed a new strategy of multienzyme-targeted fluorescent probe design (MEET-FD) and discovered a novel fluorescent probe for evaluating the extensive pesticide residues. The yielded probe, termed **3CP**, was designed to target multiple serine hydrolases, releasing a precipitating fluorochrome [named 2-(2′-hydroxyphenyl)-4(3*H*)-quinazolinone (**HPQ**)] with a large Stokes shift (130 nm) and good biocompatibility upon the enzymatic hydrolysis (Figure 1). The enzyme targets include cholinesterases [acetylcholinesterase (AChE) and butyrylcholinesterase (BChE)], chymotrypsin (Chy), and carboxylesterases [carboxylesterase 1 (CE1) and carboxylesterase 2 (CE2)]. The fluorophore **HPQ** exhibits the maximum excitation and emission wavelengths at 345 and 510 nm, respectively, and demonstrates the aggregation-induced emission (AIE) effect and nondiffuse property, making **3CP** as an effective tool for in situ real-time tracing of the residual pesticides.[32−38] This probe exhibits good detection capability for the representative organophosphorus and carbamate pesticides in live cells and zebrafish, as well as the fresh vegetables. Moreover, it achieved the rapid detection of pyrethroid pesticides for the first time on the basis of the enzyme inhibition-based principle. In all, this new probe shows promising potential for the detection of pesticide residues alone or conjugated in biodevices.

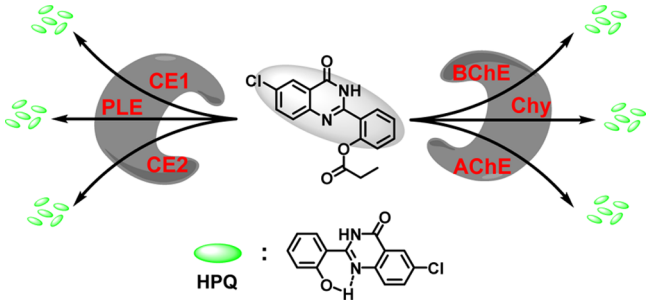

Figure 1. Recognition mechanism of the designed probe **3CP** toward the multiple metabolic serine hydrolases. AChE represents acetylcholinesterase, BChE represents butyrylcholinesterase, CE1 represents carboxylesterase 1, CE2 represents carboxylesterase 2, Chy represents chymotrypsin, and PLE represents pig liver esterase. **HPQ** refers to the fluorophore released form the enzyme-catalyzed hydrolysis of probe **3CP**.

EXPERIMENTAL SECTION

Organic Synthesis. *Reagents.* Chemical reagents were purchased from commercial companies, salicylaldehyde from Aladdin (Shanghai, China), 2-amino-5-chlorobenzamide from Bidepharm (Shanghai, China), and propionyl chloride from Energy Chemical (Shanghai, China). Solvents including acetone, petroleum, dichloromethane, dimethyl sulfoxide (DMSO), and triethylamine were purchased from Sinopharm (Beijing, China). Pesticides and other related inhibitors were of analytical grade and purchased from Sigma-Aldrich (Shanghai, China), including phenylmethylsulfonyl fluoride (PMSF), aldicarb sulfone, carbaryl, dipterex, dichlorvos, and deltamethrin. Human CE2 and CE1 were bought from the Research Institute for Liver Disease (Shanghai, China). Other enzymes, such as equine liver BChE, *Electrophorus electricus* AChE, *Streptoverticillium mobaraense* glutathione *S*-transferase, potato acid phosphatase, pig liver esterase (PLE), porcine pepsin, bovine Chy, and bovine trypsin, were obtained from Sigma-Aldrich (Shanghai, China). Unless otherwise noted, all of the starting materials were commercially available and treated with standard methods provided by the manufactures' instructions.

Instrumentation. Fluorescence spectra were recorded with a microplate reader (SpectraMax M5, Molecular Devices) using 96-well luminescent plates or quartz cuvettes (Hellma, Germany). ^{1}H NMR and ^{13}C NMR spectra for the target compounds were determined in $CDCl_3$ on an AVANCE III HD 400 or 100 MHz spectrometer, and the chemical shift (δ) is given in ppm relative to tetramethylsilane. High-resolution MS was obtained on an Agilent 6460 triple quadrupole mass spectrometer. HPLC analysis was performed with an Agilent 1260 Infinity II. Particle size distributions were acquired by Wyatt Technology DynaPro NanoStar. The fluorescence imaging was carried out by an inverted fluorescence microscope (Olympus IX71, Japan).

Synthesis of ***HPQ****.* The synthesis of **HPQ** was carried out according to the published ref 33.

Synthesis of Probe ***3CP****.* **HPQ** (136 mg, 0.5 mmol) was dissolved in 20 mL of dichloromethane. Then, 140 μL of Et_3N was added to the solution when the system was kept under stirring. After 10 min, 90 μL of propionyl chloride was added dropwise into the reaction mixture. When the reaction was completed, the crude product was acquired through vacuum distillation. Thereafter, the crude product was further purified by flash column chromatography (acetone/petroleum = 1:5) to get white powder (142 mg, 86%). ^{1}H NMR (400 MHz, $CDCl_3$): δ 10.71 (s, 1H), 8.22 (s, 1H), 8.07−7.97 (m, 1H), 7.75−7.67 (m, 2H), 7.62−7.54 (m, 1H), 7.43 (t, J = 7.3 Hz, 1H), 7.27 (d, J = 8.0 Hz 1H), 2.61 (q, J = 7.5 Hz, 2H), 1.20 (t, J = 7.5 Hz, 3H). ^{13}C NMR (101 MHz, $CDCl_3$): δ 172.30, 161.45, 150.16, 148.54, 147.56, 135.31, 133.00, 132.54, 130.51, 129.53, 126.61, 125.89, 125.74, 123.79, 121.99, 27.83, 8.88. ESI-MS m/z: calcd for $C_{17}H_{13}ClN_2O_3$ (M + Na^+), 351.0507; detected, 351.0510.

Computational Modeling. The three-dimensional structures of the corresponding compounds including the probe **3CP** were prepared by SYBYL software. The crystal structures of AChE, BChE, and CE were downloaded from the Protein Data Bank (PDB IDs: 1B41, 1MX5, and 1P0M). The AutoDock 4.2 program was used to dock the corresponding compounds into the catalytic sites of desired enzymes. The Lamarckian genetic algorithm was applied for the docking

https://doi.org/10.1021/acs.analchem.1c00553
Anal. Chem. 2021, 93, 7079−7085

conformational search. The grid size was set to 40 × 40 × 40 Å, and the grid space was set to 0.375 Å. The grid center was set to make the grid box cover the whole catalytic site. Other parameters were set as default values. Among the top 100 candidates of docked poses, the best candidate was selected according to the standard AutoDock scoring function and the yielded binding modes were analyzed accordingly.

Fluorometric Assays. The probe (**3CP**)-based fluorometric assays were carried out with the procedures described in the previous report.[39] These tests were executed with or without the inhibitors under optimized conditions (37 °C, pH 7.4, λ_{ex} = 345 nm and λ_{em} = 510 nm), unless otherwise noted. All the experiments were repeated at least three times.

Cell Culture and Live Cell Imaging. Human liver hepatocellular cells (Hep G2) were kindly provided by Procell Life Science and Technology Co. Ltd. (Wuhan, China). The cells were grown routinely in minimum essential medium (MEM, Gibco, USA) supplemented with 10% (v/v) fetal bovine serum (Gibco, USA). Hep G2 cells were seeded on confocal cell culture dishes (NEST, 15 mm) in 1.0 mL of culture medium for 24 h before imaging. After that, cells were washed with phosphate buffer saline (PBS) and then incubated with 1% DMSO or particular insecticide (50 μM, dissolved in 1% DMSO) for 1 h. Then, the probe **3CP** (20 μM) in MEM was added to each well. After washing the cells with PBS for three times, fluorescence images were then acquired with a fluorescence microscope (Olympus IX71, Japan).

Live Imaging in Zebrafish. The zebrafish were bought from Nanjing EzeRinka Biotechnology Co. Ltd. They were kept with fresh E3 medium. After the zebrafish were placed in 35 mm confocal dishes, they were treated with 100 μM insecticide for 30 min. Then, 30 μM **3CP** was added into the dish and further incubated for 20 min. Finally, the fluorescence imaging was carried out by an inverted fluorescence microscope with a 4× objective lens.

Detecting the Presence of Pesticides in Vegetables. Lettuce was selected as the sample to assess the level of dipterex residues for pesticide determination. 10 g of lettuce was cut into pieces and then to it was added 20 mL of PBS (pH = 7.4) solution. After being well shaken, the mixture was heated at 95 °C for 10 min to denature the endogenous enzymes and proteins to avoid the possible interference of the inherent enzymes. The resulting solution was then filtered through a 0.22 μm filter membrane to remove impurities. The obtained filtrate was added with CE2 (10 μg/mL) and dipterex solutions of different concentrations and incubated for 15 min. Thus, a standard curve of the inhibition rate with the concentration of dipterex was obtained. After spraying different concentrations of dipterex on lettuce, the lettuce was immediately treated according to the abovementioned method and the accurate concentration of the dipterex solution was detected by the enzyme inhibition method to calculate the recovery rates.

RESULTS AND DISCUSSION

Probe Design and Identification. The principle for the enzyme inhibition-based biosensors to detect pesticides is that pesticides inhibit the activity of a particular enzyme and hence prevent the catalysis of the substrate. The enzyme inhibition caused by the pesticides indirectly led to the change in the optical signal or electrical signal. In this scenario, a multi-enzyme-targeted fluorogenic substrate is believed to be very helpful for biosensor construction to analyze residues of wide variety of pesticides. To date, the enzyme-targeted design of two main types of small ligands, inhibitor and substrate, has triggered the extensive interest of the chemical biology community. The concept of multitarget inhibitors made rapid and spectacular progress in drug discovery and contributed numbers of approved multitarget drugs such as cariprazine for the treatment of schizophrenia and bipolar disorders.[40,41] The basic strategy for multitarget inhibitor design is combining or merging distinct frameworks into a single chemical entity, with cleavable or noncleavable linkers. However, this strategy is not applicable in designing a multitarget substrate that should be converted or broken down by multiple enzymes of interest. As a matter of fact, it was seldomly reported that the combination of recognition sites resulted in a multitarget substrate, especially for bulky fluorogenic substrates. In our understanding, it is relatively feasible to discover a common recognition site that could be catalyzed by multiple targets, and few dual enzyme-targeted substrates were published previously with this rationale. There is no report concerning the design of the fluorogenic substrate targeting three enzymes or more, not to mention the design of the multienzyme-targeted fluorogenic substrate for detecting pesticide residues.

Previously, we developed a general rationale for designing the fluorogenic substrate specifically for a particular serine hydrolase, adopting a central amide bond or ester bond flanked by a pair of fluorophore and quencher.[42,43] Directed by this consistent rationale, a solid-state fluorochrome (**HPQ**), to build the multienzyme-targeted fluorogenic substrate, was selected in this study in conjugation with a recognition group. **HPQ** is a special fluorophore that is insoluble in water due to the contribution of the intramolecular hydrogen bond[44,45] and exhibits the excited-state intramolecular proton transfer mechanism and AIE phenomenon.[36,37] Thus, the remaining challenge is how to find a common recognition group to ensure the catalytic efficiency of those major targets of insecticides, such as cholinesterases (AChE and BChE), carboxylesterases (CE1 and CE2), and Chy. To overcome this obstacle, we developed a new strategy of MEET-FD on the basis of the molecular docking and computational analysis to identify a common substrate for those hydrolases. As mentioned previously, Chy could tolerate bulky substitutions as the recognition groups because it is specific for cleaving the peptide or ester bond that is adjacent to aromatic residues.[39,46] Therefore, the challenge was simplified as to explore a common recognition group for cholinesterases and carboxylesterases. We superimposed the crystal structures of the abovementioned enzymes, human AChE (PDB entry: 1B41),[47] human BChE (PDB entry: 1P0M),[48] and CE1 (PDB entry: 1MX5).[49] The structural analysis indicates that their active sites displayed as the surface are quite different from each other, but the catalytic triads (made of the three essential amino acid residues, His, Asp, and Ser) are very conservative (Figure 2A,B). Then, a virtual probe, the formic acid ester-attached **HPQ**, was designed as a template to be docked into the active sites of those enzymes, and the complex models were analyzed accordingly. As indicated in Figure 2C, the simulated binding modes of the virtual probe in those enzymes are very similar, and more interestingly, the formic acid ester moiety of the template probe exhibits the same orientation toward the green-colored mesh area. Apparently, the green-colored mesh sphere is part of the common area shared by those interested enzymes, which suggests the accommodable steric feature of

https://doi.org/10.1021/acs.analchem.1c00553
Anal. Chem. 2021, 93, 7079−7085

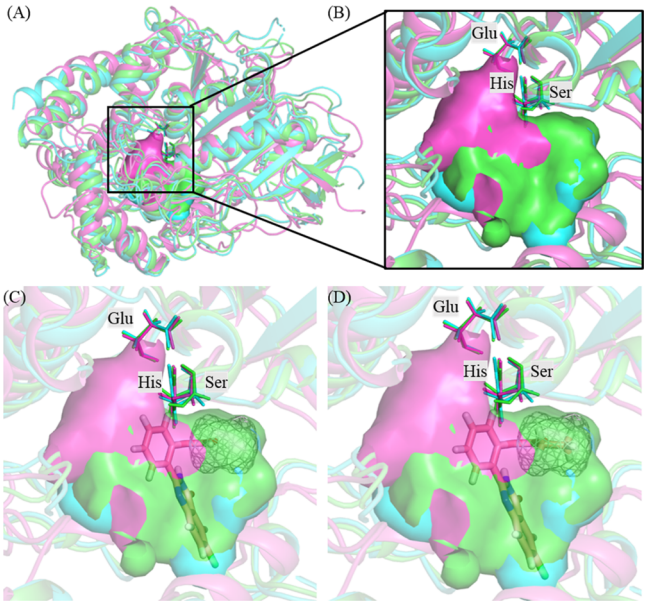

Figure 2. Simulated evolution of probe **3CP** as the common fluorogenic substrate for multiple serine hydrolases. (A) Structural superposition of the crystal structures of AChE (blue cartoon), CE1 (magenta cartoon), and BChE (green cartoon). The residues of the catalytic triad (Glu, His, and Ser) are highlighted as sticks, and the interior binding pockets are represented as surfaces. (B) Close view of the binding pockets. (C) Binding mode of the designed template probe. (D) Binding mode of the probe **3CP**. The designed probes are shown as pink sticks, and the mesh area represents the available space of the recognition groups.

the recognition group for the desirable probe. On the one hand, the lock and key theory suggests that the better the probe cavity matching, the higher will be catalytic response. On the other hand, the volume of the recognition group should not be larger than the green-colored mesh sphere (~75 Å^3) as the shared space of the active sites for those enzymes. Thus, the ethyl group with the volume of ~62.75 Å^3 was introduced to link the ester bond to fit the green-colored sphere well, yielding **3CP** as the potential multiple target-based fluorogenic substrate (Figure 2D).

Kinetic Characterization and Sensitivity for Pesticide Detection. To validate the abovementioned prediction, the probe **3CP** was successfully synthesized and the chemical structure was fully characterized (Figures S1 and S2). As expected, the entire probe is water-soluble and the fluorescence is quenched well (Figure S3). Accordingly, an "off−on" fluorescence sensing system could be established, if the ester bond was cleaved by the catalysis of hydrolase, and thus could detect the pesticide residues on the basis of the enzyme inhibition mechanism. In this regard, the response of **3CP** against each target of those enzymes (BChE, AChE, CE1, CE2, and Chy) was investigated (Figure S4). As anticipated, when incubating **3CP** with each of the hydrolases, the probe was fast hydrolyzed within 5−60 min (Figure S5), releasing free **HPQ** which started to precipitate after a very short delay, and the precipitate resulted in bright solid-state fluorescence with more than 100-fold fluorescence enhancement. After that, the test conditions including temperature and pH were optimized, and the optimal condition is 37 °C and pH 7.4 (Figures S6 and S7). It revealed that **3CP** is very stable in wide pH solution ranging from 5 to 9. Under the abovementioned reaction condition, the detection limits (S/N = 3) of this probe were determined to be 118.48 ng/mL for AChE, 82.31 ng/mL for BChE, 65.12 ng/mL for CE1, 34.15 ng/mL for CE2, 62.23 ng/mL for Chy, and 1.78 ng/mL for PLE, respectively (see Table S1 and Figure S8). Off note, HPLC analysis and particle size analysis verified the release of **HPQ** with catalysis of BChE, providing plausible proofs for the expected reaction mechanism (Figures S9 and S10). To quantify the catalytic activity of all the tested enzymes against **3CP**, we characterized the hydrolysis of **3CP** catalyzed by each enzyme (Figure S11). Accordingly, the Michaelis−Menten constants (K_m) and the catalytic rate constants (k_{cat}) were determined, and the data are listed in Table 1. Apparently, **3CP** showed micromolar level K_m values, suggesting the strong binding affinity of this fluorogenic substrate against all the tested enzymes. The abovementioned analysis reveals that **3CP** is a suitable common substrate to be applied for sensing the activity of cholinesterases, carboxylesterases, and Chy.

As mentioned before, organophosphorus, pyrethroid, and carbamate pesticides are used worldwide not only for crop protection but also for controlling infectious pests. However, the significant residues of these pesticides definitely pose a potential threat to environment and even human health. Some typical types of pesticides, dichlorvos, carbaryl, and deltamethrin, were choosed as representatives to investigate whether **3CP** could quantitatively detect the presence of pesticides. According to the European Commission website, the maximum residue levels for dichlorvos and carbaryl on vegetables are about 10 μg/L, and the maximum residue level for deltamethrin on vegetables is no more than 10 μg/L. Subsequently, taking the limit of detection (LOD) as an indicator, the sensing sensitivity of **3CP** against the abovementioned pesticides was determined separately (Table 1 and Figure S12). As depicted in Table 1, the LODs of **3CP**-based fluorometric assay toward all three pesticides are less than 10 μg/kg (a general default maximum residue level) and definitely meet the requirement of the sensitivity. Off note, CE1-inhibition-based detection with probe **3CP** reached ultrahigh sensitivity against dichlorvos, and the LOD was calculated to be ~1.14 pg/kg, which improved by about 6−7 orders of

Table 1. Kinetic Parameters of 3CP Catalyzed by the Tested Human Serine Hydrolases (AChE, BChE, CE1, CE2, and Chy), Respectively, and the Sensitivity of 3CP-Based Detection of the Representative Pesticides

	kinetic parameters			LOD		
	K_m (M)	k_{cat} (min^{-1})	k_{cat}/K_m (M^{-1}·min^{-1})	dichlorvos	carbaryl	deltamethrin (mg/L)
AChE	5.10×10^{-5}	433.44	8.50×10^{6}	5.61 μg/L	3.46 μg/L	4.95
BChE	1.58×10^{-5}	31.71	2.00×10^{6}	4.10 μg/L	4.96 μg/L	3.96
CE1	4.81×10^{-5}	19.77	4.11×10^{6}	1.14 pg/L	21.18 μg/L	3.35
CE2	6.81×10^{-5}	31.20	4.57×10^{6}	11 ng/L	0.24 μg/L	1.44
Chy	3.44×10^{-5}	15.52	4.51×10^{6}	24.4 mg/L	3.43 mg/L	4.20

https://doi.org/10.1021/acs.analchem.1c00553
Anal. Chem. 2021, 93, 7079−7085

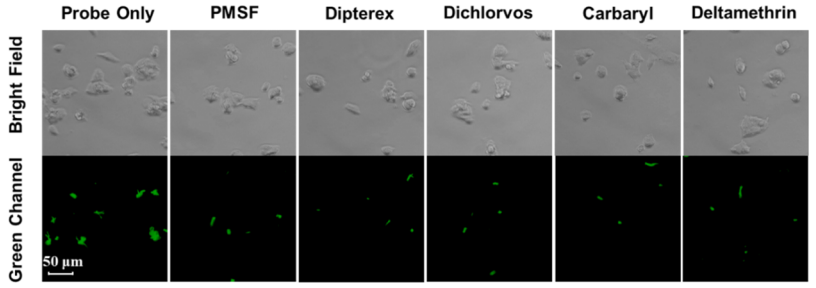

Figure 3. Fluorescence images of living Hep G2 cells treated with 20 μM probe **3CP** for 20 min in the presence and absence of pretreatment of 50 μM pesticides (dipterex, dichlorvos, deltamethrin, and carbaryl) and PMSF for 30 min.

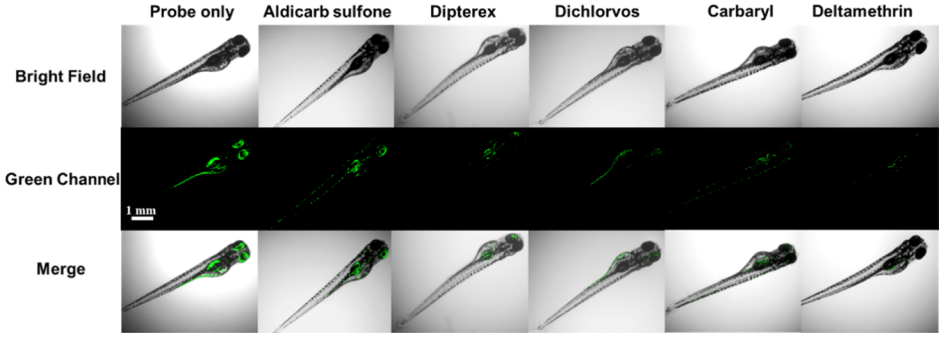

Figure 4. In vivo detection of pesticides in zebrafish by probe **3CP**. The live imaging fluorescence image was taken from zebrafish preincubated with DMSO (0.5%), dipterex, dichlorvos, aldicarb sulfone, deltamethrin, and carbaryl (100 μM) for 30 min, followed by further incubation with **3CP** (30 μM) for 20 min. The scale bar is 1 mm.

magnitude when compared with the maximum residue level claimed by European Commission. Moreover, the sensitivity of **3CP** alone for dichlorvos and carbaryl is comparable with those enzyme inhibition-based biosensors conjugated with nanomaterials (Table S2). It is worth to mention that, to our best knowledge, **3CP** is the first enzyme inhibition-based biosensor that can detect pyrethroid pesticides, although the sensitivity needs further improvement. The mechanism for pyrethroid pesticide detection with **3CP** may be thus: carboxylesterases and Chy are important metabolic enzymes for pyrethroids and can efficiently catalyze the hydrolysis of this probe. Pyrethroids are known to affect a variety of voltage- and ligand-gated ion channels.[50] Therefore, a probe targeting the ion channels may be explored for pyrethroid detection in the future. The abovementioned analysis suggests that **3CP** is generally applicable for easy and rapid detection of widely used insecticides, like organophosphorus, carbamate, and pyrethroid pesticides.

Fluorescence Imaging of Cells Pretreated with Pesticides. To illustrate the capability of the probe **3CP** for the detection of pesticide residues in living cells, we first performed a standard MTT assay in HEK293 cells with **3CP** to evaluate the potential toxicity. It was found that the cell viability was not significantly changed upon treatment with 20 μM **3CP** at 37 °C for 24 h, indicating the low cytotoxicity and good biocompatibility of this probe. Next, the probe **3CP** was applied to image the Hep G2 cells without and with preincubation with the abovementioned pesticides. It is worth to mention that PMSF, a general inhibitor for common serine hydrolases, was used as the positive control for the cellular study. This probe is anticipated to be capable of imaging pesticide residues in Hep G2 cells on the basis of the reaction with the endogenous serine hydrolases. As shown in Figure 3, cells only treated with **3CP** displayed strong green fluorescence, suggesting that endogenous serine hydrolases indeed hydrolyze **3CP** and produced the quick fluorescence response. On the contrary, preincubation with pesticides in cells significantly alleviated the fluorescence responses to different degrees. More specifically, very weak fluorescence was observed in the cells separately pretreated with deltamethrin, dipterex, dichlorvos, and carbaryl, which are very similar with that of cells treated with PMSF. It revealed that **3CP** could sense organophosphorus and carbamate pesticides in a sensitive and reliable manner. Interestingly, cells pretreated with aldicarb sulfone, a pharmacologically active metabolite but much less potent than carbamate pesticides, showed a certain decrease in the fluorescence intensity. These results show that **3CP** is a reliable platform for indicating the existence of organophosphorus and carbamate pesticides at the single-cell level.

Fluorescence Imaging of Zebrafish Pretreated with Pesticides. To further evaluate the potential of **3CP** for visualizing the pesticides in vivo, the fluorescence imaging of living zebrafish treated with probe **3CP** in the presence and absence of pesticides was carried out. As an aquatic model organism, zebrafish are usually utilized for fluorescent bioimaging in agriculture and biomedical research. In general, we exposed all the zebrafish to the probe **3CP** with and without the preincubation of the six pesticides of three types (dipterex, dichlorvos, aldicarb sulfone, deltamethrin, and carbaryl). Zebrafish themselves showed no obvious fluorescence. After treating the zebrafish only with **3CP**, strong green fluorescence could be observed throughout the zebrafish bodies, particularly the eyes and abdomen (Figure 4), and the distribution of the fluorescence signal corresponds to distribution of these enzymes.[51,52] To our delight, zebrafish pretreated with all those abovementioned pesticides, including deltamethrin, showed a much lower green fluorescence signal

https://doi.org/10.1021/acs.analchem.1c00553
Anal. Chem. 2021, 93, 7079−7085

when compared with the zebrafish treated with **3CP** alone. Among them, almost no fluorescence can be observed in zebrafish pretreated with carbaryl and deltamethrin. Collectively, these data imply that **3CP** is organism-permeable and could be regarded as a valuable visualizing tool for monitoring pesticide residues in living organisms.

Pesticide Detection in Vegetables. To test whether this quick method is workable for practical inspection of the pesticide residues in the complex matrix, we tested dipterex in the actual sample of lettuce. We believe the calibration plot obtained from the sample matrix is much more convincible to estimate the feasibility of this developed probe in practice. Some biosensors, developed by using enzymes AChE, were used to detect pesticides in fruits and vegetables.[53] Considering the overall performance of sensitivity shown in Table 1, CE2 was selected as the host enzyme to detect dipterex with probe **3CP**. In this regard, the standard curve of inhibition kinetics for the detection of various concentrations of dipterex in lettuce was obtained (Figure S13). Based on the standard curve, dipterex was quantified in the lettuce sample and the recovery rates were obtained (Table 2). It can be seen that our method has good recovery rates ranging from 90.02 to 100.29%. With all of these results taken into consideration, it can be concluded that **3CP** could be a valuable tool for pesticide detection in real samples like fruits and vegetables.

Table 2. Determination of Dipterex Concentrations in Lettuce with the 3CP-Based Detection Method

actual concentration (μg/L)	concentration of detection (μg/L)	recovery rate (%)
10	10.03 ± 1.17	100.29 ± 11.73
50	45.01 ± 1.66	90.02 ± 3.33
100	95.82 ± 4.76	95.82 ± 4.76

CONCLUSIONS

In summary, a new approach of MEET-FD was developed to rationally design a fluorogenic substrate (**3CP**) as an universal biosensor to detect the five common metabolic serine hydrolases (AChE, BChE, CE1, CE2, and Chy) simultaneously, thus indicating the residues of pesticides like organophosphorus, carbamates, and pyrethroids. The **3CP**-based sensing system achieved the visible indication of pesticide exposure in live cells and zebrafish and the sensitive detection of organophosphorus pesticides in fresh vegetables. To the best of our knowledge, **3CP** is the first enzyme-based sensor that enabled the spatiotemporal detection of pyrethroids in solution. Furthermore, the MEET-FD strategy is generally applicable to the identification of other multienzyme-responsive fluorescent probes for pesticide residue detection and other similar purposes.

ASSOCIATED CONTENT

Supporting Information

The Supporting Information is available free of charge at https://pubs.acs.org/doi/10.1021/acs.analchem.1c00553.

Chemical structure characterization, HPLC analysis, and kinetic figures and tables for characterization of the developed probe (PDF)

AUTHOR INFORMATION

Corresponding Authors

Wen-Chao Yang − *Key Laboratory of Pesticide & Chemical Biology of Ministry of Education, International Joint Research Center for Intelligent Biosensor Technology and Health, College of Chemistry, Central China Normal University, Wuhan 430079, P. R. China;* orcid.org/0000-0002-6722-0441; Phone: 86-27-67867706; Email: tomyang@mail.ccnu.edu.cn; Fax: 86-27-67867141

Guang-Fu Yang − *Key Laboratory of Pesticide & Chemical Biology of Ministry of Education, International Joint Research Center for Intelligent Biosensor Technology and Health, College of Chemistry, Central China Normal University, Wuhan 430079, P. R. China;* orcid.org/0000-0003-4384-2593; Phone: 86-27-67867800; Email: gfyang@mail.ccnu.edu.cn; Fax: 86-27-67867141

Authors

Wu-Yingzheng Guo − *Key Laboratory of Pesticide & Chemical Biology of Ministry of Education, International Joint Research Center for Intelligent Biosensor Technology and Health, College of Chemistry, Central China Normal University, Wuhan 430079, P. R. China*

Yi-Xuan Fu − *Key Laboratory of Pesticide & Chemical Biology of Ministry of Education, International Joint Research Center for Intelligent Biosensor Technology and Health, College of Chemistry, Central China Normal University, Wuhan 430079, P. R. China*

Shi-Yu Liu − *Key Laboratory of Pesticide & Chemical Biology of Ministry of Education, International Joint Research Center for Intelligent Biosensor Technology and Health, College of Chemistry, Central China Normal University, Wuhan 430079, P. R. China*

Long-Can Mei − *Key Laboratory of Pesticide & Chemical Biology of Ministry of Education, International Joint Research Center for Intelligent Biosensor Technology and Health, College of Chemistry, Central China Normal University, Wuhan 430079, P. R. China*

Yao Sun − *Key Laboratory of Pesticide & Chemical Biology of Ministry of Education, International Joint Research Center for Intelligent Biosensor Technology and Health, College of Chemistry, Central China Normal University, Wuhan 430079, P. R. China;* orcid.org/0000-0002-6519-7436

Jun Yin − *Key Laboratory of Pesticide & Chemical Biology of Ministry of Education, International Joint Research Center for Intelligent Biosensor Technology and Health, College of Chemistry, Central China Normal University, Wuhan 430079, P. R. China;* orcid.org/0000-0003-4732-6123

Complete contact information is available at: https://pubs.acs.org/10.1021/acs.analchem.1c00553

Author Contributions

†W.-Y.G. and Y.-X.F. made equal contributions.

Notes

The authors declare no competing financial interest.

ACKNOWLEDGMENTS

This research was supported by the National Key R&D Program (2017YFA0505203), the National Natural Science Foundation of China (nos. 21977036 and U20A2038), and Hubei Province Natural Science Foundation (nos. 2018CFA072 and 2020BHB027).

REFERENCES

(1) Vinet, L.; Zhedanov, A. *J. Phys. A: Math. Theor.* **2011**, *44*, 085201.
(2) Winter, C. K. *J. Agric. Food Chem.* **2012**, *60*, 4425−4429.
(3) Cabras, P.; Angioni, A. *J. Agric. Food Chem.* **2000**, *48*, 967−973.
(4) Fantke, P.; Juraske, R. *Environ. Sci. Technol.* **2013**, *47*, 3548−3562.
(5) Jallow, M. F. A.; Awadh, D. G.; Albaho, M. S.; Devi, V. Y.; Thomas, B. M. *Sci. Total Environ.* **2017**, *574*, 490−498.
(6) Eddleston, M.; Buckley, N. A.; Eyer, P.; Dawson, A. H. *Lancet* **2008**, *371*, 597−607.
(7) Kaur, J.; Singh, P. K. *Phys. Chem. Chem. Phys.* **2020**, *22*, 15105−15119.
(8) Seiber, J. N.; Kleinschmidt, L. A. *J. Agric. Food Chem.* **2011**, *59*, 7536−7543.
(9) Cao, J.; Wang, M.; Yu, H.; She, Y.; Cao, Z.; Ye, J.; Abd El-Aty, A. M.; Hacımüftüoğlu, A.; Wang, J.; Lao, S. *J. Agric. Food Chem.* **2020**, *68*, 7298−7315.
(10) Lehotay, S. J.; Cook, J. M. *J. Agric. Food Chem.* **2015**, *63*, 4395−4404.
(11) Hengel, M. J.; Wong, J. W.; Redman, Z. C.; Rering, C.; Williams, K. L. *J. Chem. Educ.* **2020**, *97*, 226−233.
(12) Wong, J. W.; Wang, J.; Chow, W.; Carlson, R.; Jia, Z.; Zhang, K.; Hayward, D. G.; Chang, J. S. *J. Agric. Food Chem.* **2018**, *66*, 9573−9581.
(13) Maguire, W. J.; Call, C. W.; Cerbu, C.; Jambor, K. L.; Benavides-Montes, V. E. *J. Agric. Food Chem.* **2019**, *67*, 12670−12674.
(14) Shalini Devi, K. S.; Anusha, N.; Raja, S.; Senthil Kumar, A. *ACS Appl. Nano Mater.* **2018**, *1*, 4110−4119.
(15) Nasir, M. Z. M.; Mayorga-Martinez, C. C.; Sofer, Z.; Pumera, M. *ACS Nano* **2017**, *11*, 5774−5784.
(16) Sahoo, D.; Mandal, A.; Mitra, T.; Chakraborty, K.; Bardhan, M.; Dasgupta, A. K. *J. Agric. Food Chem.* **2018**, *66*, 414−423.
(17) Greenwald, E. C.; Mehta, S.; Zhang, J. *Chem. Rev.* **2018**, *118*, 11707−11794.
(18) Chernov, K. G.; Redchuk, T. A.; Omelina, E. S.; Verkhusha, V. V. *Chem. Rev.* **2017**, *117*, 6423−6446.
(19) Mcconnell, E. M.; Cozma, I.; Morrison, D.; Li, Y. *Anal. Chem.* **2020**, *92*, 327−344.
(20) Kwok, R. T. K.; Leung, C. W. T.; Lam, J. W. Y.; Tang, B. Z. *Chem. Soc. Rev.* **2015**, *44*, 4228−4238.
(21) Li, D.; Li, Z.; Chen, W.; Yang, X. *J. Agric. Food Chem.* **2017**, *65*, 4209−4215.
(22) Li, H.; Su, D.; Gao, H.; Yan, X.; Kong, D.; Jin, R.; Liu, X.; Wang, C.; Lu, G. *Anal. Chem.* **2020**, *92*, 3198−3205.
(23) Zhu, Y.; Wu, J.; Han, L.; Wang, X.; Li, W.; Guo, H.; Wei, H. *Anal. Chem.* **2020**, *92*, 7444−7452.
(24) Liu, X.; Song, M.; Hou, T.; Li, F. *ACS Sens.* **2017**, *2*, 562−568.
(25) Korram, J.; Dewangan, L.; Karbhal, I.; Nagwanshi, R.; Vaishanav, S. K.; Ghosh, K. K.; Satnami, M. L. *RSC Adv.* **2020**, *10*, 24190−24202.
(26) Chen, C.; Tian, R.; Zeng, Y.; Chu, C.; Liu, G. *Bioconjugate Chem.* **2020**, *31*, 276−292.
(27) Singh, H.; Tiwari, K.; Tiwari, R.; Pramanik, S. K.; Das, A. *Chem. Rev.* **2019**, *119*, 11718−11760.
(28) Liu, S.-Y.; Qu, R.-Y.; Li, R.-R.; Yan, Y.-C.; Sun, Y.; Yang, W.-C.; Yang, G.-F. *Anal. Chem.* **2020**, *92*, 9205−9213.
(29) Wu, L.; Huang, C.; Emery, B. P.; Sedgwick, A. C.; Bull, S. D.; He, X.-P.; Tian, H.; Yoon, J.; Sessler, J. L.; James, T. D. *Chem. Soc. Rev.* **2020**, *49*, 5110−5139.
(30) Guan, P.; Liu, Y.; Yang, B.; Wu, Y.; Chai, J.; Wen, G.; Liu, B. *Talanta* **2021**, *225*, 121948.
(31) Liu, H.-W.; Li, K.; Hu, X.-X.; Zhu, L.; Rong, Q.; Liu, Y.; Zhang, X.-B.; Hasserodt, J.; Qu, F.-L.; Tan, W. *Angew. Chem., Int. Ed.* **2017**, *56*, 11788−11792.
(32) Prost, M.; Canaple, L.; Samarut, J.; Hasserodt, J. *ChemBioChem* **2014**, *15*, 1413−1417.
(33) Zhou, L.; Peng, Y.; Wang, Q.; Lin, Q. *J. Photochem. Photobiol., B* **2017**, *167*, 264−268.
(34) Zhou, Y.; Liu, M.-M.; Li, J.-Y.; Ye, M.-A.; Yao, C. *Dyes Pigm.* **2018**, *158*, 277−284.
(35) Ou-Yang, J.; Li, Y.-F.; Wu, P.; Jiang, W.-L.; Liu, H.-W.; Li, C.-Y. *ACS Sens.* **2018**, *3*, 1354−1361.
(36) Gao, M.; Li, S.; Lin, Y.; Geng, Y.; Ling, X.; Wang, L.; Qin, A.; Tang, B. Z. *ACS Sens.* **2016**, *1*, 179−184.
(37) Yang, W.; Zhao, X.; Zhang, J.; Zhou, Y.; Fan, S.; Sheng, H.; Cao, Y.; Hu, Y. *Dyes Pigm.* **2018**, *156*, 100−107.
(38) Li, K.; Hu, X.-X.; Liu, H.-W.; Xu, S.; Huan, S.-Y.; Li, J.-B.; Deng, T.-G.; Zhang, X.-B. *Anal. Chem.* **2018**, *90*, 11680−11687.
(39) Wu, L.; Yang, S.-H.; Xiong, H.; Yang, J.-Q.; Guo, J.; Yang, W.-C.; Yang, G.-F. *Anal. Chem.* **2017**, *89*, 3687−3693.
(40) Korcsmáros, T.; Szalay, M. S.; Böde, C.; Kovács, I. A.; Csermely, P. *Expert Opin. Drug Discovery* **2007**, *2*, 799−808.
(41) Ramsay, R. R.; Popovic-Nikolic, M. R.; Nikolic, K.; Uliassi, E.; Bolognesi, M. L. *Clin. Transl. Med.* **2018**, *7*, No. e3.
(42) Liu, S.-Y.; Xiong, H.; Li, R.-R.; Yang, W.-C.; Yang, G.-F. *Anal. Chem.* **2019**, *91*, 3877−3884.
(43) Liu, S.-Y.; Xiong, H.; Yang, J.-Q.; Yang, S.-H.; Li, Y.; Yang, W.-C.; Yang, G.-F. *ACS Sens.* **2018**, *3*, 2118−2128.
(44) Diwu, Z.; Klaubert, D. H.; Haugland, R. P. Spectral Properties and Biological Applications of ELF Enzyme Substrates That Yield Fluorescent Precipitates at the Enzymatic Activity Sites. *Advances in Fluorescence Sensing Technology IV*; International Society for Optics and Photonics, 1999; Vol. *3602*, pp 265−274.
(45) Zhang, X.-b.; Waibel, M.; Hasserodt, J. *Chem.—Eur. J.* **2010**, *16*, 792−795.
(46) Xiong, H.; Li, R.-R.; Liu, S.-Y.; Wu, F.-X.; Yang, W.-C.; Yang, G.-F. *ACS Appl. Bio Mater.* **2018**, *1*, 310−317.
(47) Kryger, G.; Harel, M.; Giles, K.; Toker, L.; Velan, B.; Lazar, A.; Kronman, C.; Barak, D.; Ariel, N.; Shafferman, A.; Silman, I.; Sussman, J. L. *Acta Crystallogr., Sect. D: Biol. Crystallogr.* **2000**, *56*, 1385−1394.
(48) Nicolet, Y.; Lockridge, O.; Masson, P.; Fontecilla-Camps, J. C.; Nachon, F. *J. Biol. Chem.* **2003**, *278*, 41141−41147.
(49) Bencharit, S.; Morton, C. L.; Xue, Y.; Potter, P. M.; Redinbo, M. R. *Nat. Struct. Biol.* **2003**, *10*, 349−356.
(50) Soderlund, D. M. *Toxicology and Mode of Action of Pyrethroid Insecticides*, 3rd ed.; Elsevier Inc., 2010; Vol. *2*.
(51) Ma, Y.; Gao, W.; Ma, S.; Liu, Y.; Lin, W. *Anal. Chem.* **2020**, *92*, 13405−13410.
(52) Wang, J.; Teng, Z.; Zhang, L.; Yang, Y.; Qian, J.; Cao, T.; Cao, Y.; Qin, W.; Liu, Y.; Guo, H. *ACS Sens.* **2020**, *5*, 3264−3273.
(53) Liu, D.; Chen, W.; Wei, J.; Li, X.; Wang, Z.; Jiang, X. *Anal. Chem.* **2012**, *84*, 4185−4191.

https://doi.org/10.1021/acs.analchem.1c00553
Anal. Chem. 2021, 93, 7079−7085